EasyChair Preprint

№ 8135

An Integrated Localization Method for Mixed Near-Field and Far-Field Sources Based on Mixed-Order Statistic

Xile Li, Yangming Lai, Shixing Yang and Wei Yi

May 31, 2022

An Integrated Localization Method for Mixed Near-Field and Far-Field Sources Based on Mixed-order Statistic

Xile Li, Yangming Lai, Shixing Yang and Wei Yi
University of Electronic Science and Technology of China
Chengdu 611731, China
Email: luestcer@gmail.com, ymlaiuestc@163.com, yangshixing@std.uestc.edu.cn and kussoyi@gmail.com

***Abstract*—This paper considers the integrated localization for the mixed near-field (NF) and far-field (FF) sources using the uniform linear array (ULA). With the help of the polynomial rooting methods and the propagator, an efficient algorithm is proposed to provide an integrated estimation of the direction of arrival (DOA) and the ranges of the sources. It takes low computational burden without the requirements that separating the DOA and range information or pre-classification of the sources. We first construct two special fourth-order cumulant matrices using the received array data, then extract the prior-electrical parameters related to the array elements by its steering matrix, and finally carry out parameter matching and classification. Besides, the proposed algorithm eliminates the need for tedious eigenvalue decomposition and spectral search steps, and has almost no aperture loss. Eventually, several simulation results show that the proposed algorithm has lower computational complexity under an acceptable accuracy, compared to the state-of-the-art methods.**

***Index Terms*—Sources localization, array signal processing, mixed sources, mixed-order statistic.**

I. Introduction

Sources localization using sensor arrays is already an important part of array signal processing for many applications such as sonar, radar and microphone arrays [1]. Up to now, many literatures investigate the direction of arrival (DOA) estimation of far field sources (FFSs) which satisfy ideal FF conditions [2]–[5], or the localization of the near-field sources (NFSs) [6]–[10]. However, when the FFSs and the NFSs coexist, the above algorithms may fail or miscalculate in some practical applications such as the speaker localization in a microphone array [11].

To deal with this issue, many effective methods have been proposed. The two-stage MUSIC algorithm (TSMUSIC) in [11] utilizes the high degree of freedom characteristics of the fourth-order cumulant, but the spectral search and eigenvalue decomposition (EVD) of cumulant matrices have a huge computational burden [12]. To reduce the computational complexity, an oblique projection method based on the second-order statistics (MBODS) was proposed in [12], which utilizes the anti-diagonal elements in the covariance matrix. Based on the MBODS, a rooting algorithm and an idea using second-order statistics without oblique projection were proposed in [13] and [14], respectively. The former avoids spectral search and the latter improves the estimation accuracy. A method that constructs three fourth-order cumulant matrices was proposed in [15], which divides a linear array into two arrays with different centers, and locating according to the geometric relationship. Another commonly used approach, known as the spatial difference method was proposed in [16], [17], which utilizes the property that the receiving covariance matrix of the FFSs is a Toeplitz conjugate symmetric matrix. In addition, the higher-order difference algorithms separate FF and NF sources through differential construction and transformation [18], [19]. The work in [20] utilizes the pseudo-orthogonality between the steering vectors of the fourth-order cumulant matrix by using mixed order statistics (MOS). Also, the propagation operator and QR decomposition were used in [21] to estimate the oblique projection operator and eliminate the FFSs from the received signals.

However, all the above algorithms either separate the DOA and range information of the sources, or estimate the parameters of FFSs and NFSs separately. The former may lead to the detection of false sources in special scenarios (for example, the sources of the FF and NF share the same DOA), while the latter requires pre-classification of the sources before the estimation. Moreover, the above algorithms need to use spectral search or EVD in application, which has a huge computational burden.

In this paper, we propose a novel mixed-order-based integrated localization method (IMOS). Unlike the MOS-based method [20], IMOS does not need to perform eigenvalue decomposition or spectral search on the covariance matrix, and does not need to approximate the kurtosis of the cumulant matrix. We first construct two cumulant matrices rationally, then extract the information of DOAs and ranges of all sources from the cumulant matrices integrally, which neither estimates the DOA and range of the source separately nor pre-classifies the sources. Moreover, by using the propagator and rooting method, the proposed algorithm avoids spectral search and EVD, therefore requires a lower computational burden in real-time signal processing applications.

II. Model and Preconditions

Assume that there are K narrowband and independent sources (FFSs or NFSs). The signals transmitted by these

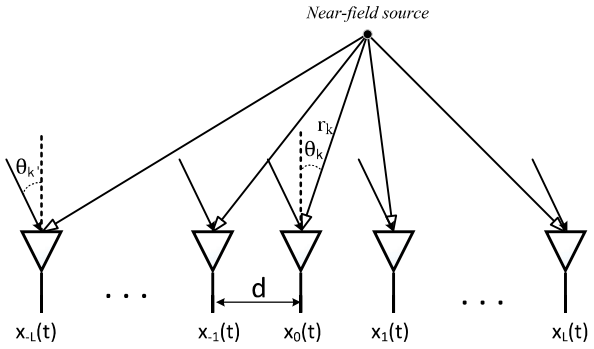

Figure 1. Uniform linear sensor array and the propagations of signals

sources impinge on a symmetric uniform linear array (ULA) with $N = 2L+1$ sensors and distance d between two adjacent sensors, as shown in Fig. 1. The sensors are labeled from $-L$ to L, and let the center of the array (the sensor labeled as 0) be the phase reference point. Then, the signal received by the lth sensor at time index t has the following form as [11],

$$x_l(t) = \sum_{k=1}^{K} s_k(t) e^{j\tau_{lk}} + n_l(t), \tag{1}$$

where $-L \le l \le L$, $t = 1, \ldots, T$, and T is the number of snapshots. The $s_k(t)$ denotes the kth source signal waveform, $n_l(t)$ represents the lth sensor noise, and τ_{lk} is the phase shift from the kth source to the lth sensor due to propagation delay, which has the following form

$$\tau_{lk} \approx l\gamma_k + l^2\phi_k, \tag{2}$$

Here, the electric angles γ_k and ϕ_k are given by

$$\gamma_k = -\frac{2\pi d}{\lambda} \sin\theta_k, \tag{3}$$

and

$$\phi_k = \frac{\pi d^2}{\lambda r_k} \cos^2\theta_k, \tag{4}$$

respectively, where λ is the wavelength, $\theta_k \in [-\pi/2, \pi/2]$ denotes the DOA of the kth source, and r_k is the range of the kth source.

Then, the receive array data in (1) can be rewritten in a matrix form,

$$\boldsymbol{x}(t) = \boldsymbol{A}\boldsymbol{s}(t) + \boldsymbol{n}(t), \tag{5}$$

where $x(t)$ and $n(t)$ are $(2L+1) \times 1$ complex vectors,

$$\boldsymbol{x}(t) = [\boldsymbol{x}_{-L}(t), ..., \boldsymbol{x}_0(t), ..., \boldsymbol{x}_L(t)]^\top, \tag{6}$$

$$\boldsymbol{n}(t) = [\boldsymbol{n}_{-L}(t), ..., \boldsymbol{n}_0(t), ..., \boldsymbol{n}_L(t)]^\top, \tag{7}$$

and steering matrix $\boldsymbol{A}$ and sources vector $\boldsymbol{s}(t)$ can be written as

$$\boldsymbol{A} = [\boldsymbol{a}(\gamma_1, \phi_1) \cdots \boldsymbol{a}(\gamma_{K_N}, \phi_{k_N}) \cdots \boldsymbol{a}(\gamma_K, \phi_K)], \tag{8}$$

$$\boldsymbol{s}(t) = [\boldsymbol{s}_1(t) \cdots \boldsymbol{s}_{K_N}(t), \boldsymbol{s}_{K_N+1}(t) \cdots \boldsymbol{s}_K(t)]^\top, \tag{9}$$

respectively, where

$$\boldsymbol{a}(\gamma_k, \phi_k) = [e^{j(-L\gamma_k + L^2\phi_k)}, ..., 1, ..., e^{j(L\gamma_k + L^2\phi_k)}]^\top, \tag{10}$$

and K_N represents the number of NFSs that lie in Fresnel region, i.e., $r_k \in [0.62(D^3/\lambda)^{1/2}, 2D^2/\lambda]$ in K sources. Here, $D = 2Ld$ represents the array aperture.

For the rest of the paper, the following basic assumptions are required as [9], [15], [18], [20]:

Assumption 1. The array has been well calibrated, to avoid phase ambiguity, the distance d between two adjacent sensors of the uniform linear array satisfies the relation $d \le \lambda/4$.

Assumption 2. The signals $\{s_k(t)\}_{k=1}^K$ are mutually statistically independent, complex non-Gaussian fourth-order narrowband stationary processes with nonzero kurtosis.

Assumption 3. The sensor noises $\{n_l(t)\}_{l=1}^L$ are zero-mean, additive (white or color) Gaussian processes with variance σ_n^2 and statistically independent from the impinging sources.

Assumption 4. The number of all sources K is assumed to be known, the numbers of FFSs or NFSs are unknown.

III. Proposed Method

In this part, we develop a new method for mixed FFSs and NFSs localization using mixed-order statistics. In order to locate the sources, it is necessary to represent the DOA and range information of the sources in matrix forms that can be solved from the array data at first. We use the high degree of freedom of the fourth-order statistics to *construct two special cumulant matrices*. According to (3) and (4), we can evaluate the DOAs and ranges of sources by estimating γ_k and ϕ_k. Several methods evaluate γ_k from the cumulant matrix directly [11], [15], [20], [22], [23], which will cause the loss of the information of ϕ_k and make it difficult to estimate later. Then, we *extract the prior information of DOAs and ranges* of all sources from the cumulant matrices and make an integrated estimation. Finally, The *matching and classification* are arranged by using the second-order statistics. Moreover, the use of propagator can avoid eigenvalue decomposition without losing accuracy and save computing resources [24].

A. Construction of Two Special Cumulant Matrices

Based on the data model and assumptions, we first define the fourth-order cumulant using array outputs as follows [11], [20], [22],

$$\begin{aligned}
&\operatorname{cum}\left\{x_m(t), x_n^*(t), x_p^*(t), x_q(t)\right\} \\
&= \operatorname{cum}\left\{\sum_{k=1}^{K} s_k(t) e^{j\left(m\gamma_k + m^2\phi_k\right)}, \left(\sum_{k=1}^{K} s_k(t) e^{j\left(n\gamma_k + n^2\phi_k\right)}\right)^*,\right. \\
&\qquad \left.\left(\sum_{k=1}^{K} s_k(t) e^{j\left(p\gamma_k + p^2\phi_k\right)}\right)^*, \sum_{k=1}^{K} s_k(t) e^{j\left(q\gamma_k + q^2\phi_k\right)}\right\} \\
&= \sum_{k=1}^{K} e^{j\left\{[(m-n)-(p-q)]\gamma_k + \left[\left(m^2-n^2\right)-\left(p^2-q^2\right)\right]_k\right\}} \\
&\qquad \times \operatorname{cum}\left\{s_k(t), {s_k}^*(t), {s_k}^*(t), s_k(t)\right\}
\end{aligned}$$

$$= \sum_{k=1}^{K} c_{4,s_k} e^{j[(m-n)-(p-q)]\gamma_k + [(m^2-n^2)-(p^2-q^2)]\phi_k}\}. \quad (11)$$

In (11), there is no need to consider the noise component because the cumulant of Gaussian noise is equal to zero when the order greater than 2. Here, c_{4,s_k}=cum$\{s_k(t), {s_k}^*(t), {s_k}^*(t), s_k(t)\}$ is the kurtosis of the kth source.

Based on (11), we denote by u and v the labels of the sensors, and let $u, v \in [-L+1, L-1]$. We use array outputs to construct two new cumulants as

$$\begin{aligned} &\text{cum}\left\{x_u(t), x^*_{1-u}(t), x^*_v(t), x_{1-v}(t)\right\} \\ &\quad = \sum_{k=1}^{K} c_{4,s_k} e^{j2u(\gamma_k+\phi_k)} \left(e^{j2v(\gamma_k+\phi_k)}\right)^*, \quad (12) \\ &\text{cum}\left\{x_u(t), x^*_{-1-u}(t), x^*_v(t), x_{-1-v}(t)\right\} \\ &\quad = \sum_{k=1}^{K} c_{4,s_k} e^{j2u(\gamma_k-\phi_k)} \left(e^{j2v(\gamma_k-\phi_k)}\right)^*. \quad (13) \end{aligned}$$

Let $\overline{u} = u + L \in [1, 2L-1]$ and $\overline{v} = v + L \in [1, 2L-1]$, then we construct two special cumulant matrices $\boldsymbol{C}_1 \in \mathbb{C}^{(2L-1)\times(2L-1)}$ and $\boldsymbol{C}_2 \in \mathbb{C}^{(2L-1)\times(2L-1)}$ which contain both the DOAs and the distances information of sources. The $(\overline{u}, \overline{v})$th element of $\boldsymbol{C}_1$ and $\boldsymbol{C}_2$ have the following form

$$\begin{aligned} \boldsymbol{C}_1(\overline{u}, \overline{v}) &= \text{cum}\left\{x_{\overline{u}-L}(t), x^*_{1-\overline{u}+L}(t), x^*_{\overline{v}-L}(t), x_{1-\overline{v}+L}(t)\right\} \\ &= \sum_{k=1}^{K} c_{4,s_k} e^{j2(\overline{u}-L)(\gamma_k+\phi_k)} \left(e^{j2(\overline{v}-L)(\gamma_k+\phi_k)}\right)^*, \end{aligned} \quad (14)$$

$$\begin{aligned} \boldsymbol{C}_2(\overline{u}, \overline{v}) &= \text{cum}\left\{x_{\overline{u}-L}(t), x^*_{-1-\overline{u}+L}(t), x^*_{\overline{v}-L}(t), x_{-1-\overline{v}+L}(t)\right\} \\ &= \sum_{k=1}^{K} c_{4,s_k} e^{j2(\overline{u}-L)(\gamma_k-\phi_k)} \left(e^{j2(\overline{v}-L)(\gamma_k-\phi_k)}\right)^*. \end{aligned} \quad (15)$$

Based on *Assumption* 2, the cumulant matrices $\boldsymbol{C}_1$ and $\boldsymbol{C}_2$ can be written in the matrix form as

$$\boldsymbol{C}_1 = \boldsymbol{B}_1 \boldsymbol{C}_{4,5} \boldsymbol{B}_1^H, \quad (16)$$

and

$$\boldsymbol{C}_2 = \boldsymbol{B}_2 \boldsymbol{C}_{4,5} \boldsymbol{B}_2^H, \quad (17)$$

where $\boldsymbol{C}_{4,s} = \text{diag}\left[c_{4,s_1}, \ldots, c_{4,s_r}\right] \in \mathbb{R}^{K\times K}$, $\boldsymbol{B}_1 = \left[\boldsymbol{b}_1(\theta_1, r_1), \ldots, \boldsymbol{b}_1(\theta_K, r_K)\right] \in \mathbb{C}^{(2L-1)\times K}$ and $\boldsymbol{B}_2 = \left[\boldsymbol{b}_2(\theta_1, r_2), \ldots, \boldsymbol{b}_2(\theta_K, r_K)\right] \in \mathbb{C}^{(2L-1)\times K}$ are virtual steering matrices with

$$\boldsymbol{b}_1(\theta_k, r_k) = \left[e^{-j2(L-1)(\gamma_k+\phi_k)}, ..., e^{j2(L-1)(\gamma_k+\phi_k)}\right]^\top, \quad (18)$$

$$\boldsymbol{b}_2(\theta_k, r_k) = \left[e^{-j2(L-1)(\gamma_k-\phi_k)}, ..., e^{j2(L-1)(\gamma_k-\phi_k)}\right]^\top. \quad (19)$$

It is noted that, the two types of sources cannot be distinguished by γ_k when the FFSs and NFSs share the same DOAs, which results in the rank reduction of the steering matrix [20], [22], [23], i.e., $rank(\boldsymbol{B}) < K$. However, the steering matrix is related to both ranges and DOAs of our work, which avoids this problem.

B. Extract the Prior Information of DOAs and Ranges

The methods in [11], [15], [20], [22], [23] implement EVD to separate the main eigenvalues from all eigenvalues to get the corresponding eigenvectors, then the MUSIC or ESPRIT is employed to make estimations. However, the calculation of the eigenvalues is computationally complex and time consuming in some applications when the number of the sensors is large [21], [24], [25]. In this part, we employ the propagator method to avoid implementing EVD.

Assume that $K < 2L-1$, then we divide $\boldsymbol{C}_1$, $\boldsymbol{C}_2$ and corresponding steering matrices $\boldsymbol{B}_1$, $\boldsymbol{B}_2$ as follows,

$$\boldsymbol{C}_1 = [\overbrace{\boldsymbol{C}_{1,1}}^{K}, \overbrace{\boldsymbol{C}_{1,2}}^{2L-1-K}], \qquad \boldsymbol{C}_2 = [\overbrace{\boldsymbol{C}_{2,1}}^{K}, \overbrace{\boldsymbol{C}_{2,2}}^{2L-1-K}], \quad (20)$$

$$\boldsymbol{B}_1 = [\overbrace{\boldsymbol{B}_{1,1}}^{K}, \overbrace{\boldsymbol{B}_{1,2}}^{2L-1-K}]^\top, \quad \boldsymbol{B}_2 = [\overbrace{\boldsymbol{B}_{2,1}}^{K}, \overbrace{\boldsymbol{B}_{2,2}}^{2L-1-K}]^\top, \quad (21)$$

where $\boldsymbol{B}_{1,1} \in \mathbb{C}^{K\times K}$ and $\boldsymbol{B}_{2,1} \in \mathbb{C}^{K\times K}$ contain the first K rows of $\boldsymbol{B}_1$ and $\boldsymbol{B}_2$, respectively. We can get two linear operators $\boldsymbol{P}_1$ and $\boldsymbol{P}_2$ equivalently defined as follows,

$$\boldsymbol{B}_{1,2} = \boldsymbol{P}_1^H \boldsymbol{B}_{1,1}, \qquad \boldsymbol{B}_{2,2} = \boldsymbol{P}_2^H \boldsymbol{B}_{2,1}, \quad (22)$$

$$\boldsymbol{C}_{1,2} = \boldsymbol{C}_{1,1} \boldsymbol{P}_1, \qquad \boldsymbol{C}_{2,2} = \boldsymbol{C}_{2,1} \boldsymbol{P}_2, \quad (23)$$

and we can get the following relation as

$$\begin{aligned} \boldsymbol{Q}_1^H \boldsymbol{B}_1 &= \boldsymbol{O}_{(2L-1-K)\times K}, \\ \boldsymbol{Q}_2^H \boldsymbol{B}_2 &= \boldsymbol{O}_{(2L-1-K)\times K}, \end{aligned} \quad (24)$$

where $\boldsymbol{Q}_1 = \left[\boldsymbol{P}_1^\top, -\boldsymbol{I}_{2L-1-K}\right]^\top$, $\boldsymbol{Q}_2 = \left[\boldsymbol{P}_2^\top, -\boldsymbol{I}_{2L-1-K}\right]^\top$, $\boldsymbol{P}_1 = \left(\boldsymbol{C}_{1,1}^H \boldsymbol{C}_{1,1}\right)^{-1} \boldsymbol{C}_{1,1}^H \boldsymbol{C}_{1,2}$, and $\boldsymbol{P}_2 = \left(\boldsymbol{C}_{2,1}^H \boldsymbol{C}_{2,1}\right)^{-1} \boldsymbol{C}_{2,1}^H \boldsymbol{C}_{2,2}$. Here we set the relations for convenience as

$$\alpha_k = \gamma_k + \phi_k, \qquad \beta_k = \gamma_k - \phi_k. \quad (25)$$

The ranges and DOAs of all sources can be calculated from the prior information α_k and β_k after matching. Obviously, $\boldsymbol{b}_1(\theta_k, r_k)$ and $\boldsymbol{b}_2(\theta_k, r_k)$ are functions of α_k and β_k, respectively. The α_k and β_k can be estimated from $\boldsymbol{C}_1$ and $\boldsymbol{C}_2$ through minimizing the cost function

$$f_1(\alpha) = \boldsymbol{b}_1^H(\alpha) \boldsymbol{Q}_1 \left(\boldsymbol{Q}_1^H \boldsymbol{Q}_1\right)^{-1} \boldsymbol{Q}_1^H \boldsymbol{b}_1(\alpha), \quad (26)$$

and

$$f_2(\beta) = \boldsymbol{b}_2^H(\beta) \boldsymbol{Q}_2 \left(\boldsymbol{Q}_2^H \boldsymbol{Q}_2\right)^{-1} \boldsymbol{Q}_2^H \boldsymbol{b}_2(\beta). \quad (27)$$

C. Matching and Classification

Since the α_k and β_k are estimated, a pairing and classifying procedure which calculates the ranges and DOAs of all sources at the same time is shown below.

1) Construct and partition the array covariance matrix $\boldsymbol{R} \in \mathbb{C}^{(2L+1)\times(2L+1)}$ which is given by

$$\boldsymbol{R} = \boldsymbol{E}\left\{\boldsymbol{x}(t)\boldsymbol{x}^H(t)\right\} = \boldsymbol{A}\boldsymbol{E}\left\{s(t)\boldsymbol{s}^H(t)\right\}\boldsymbol{A}^H + \sigma_n^2 \boldsymbol{I}, \quad (28)$$

and

$$\boldsymbol{R} = [\overbrace{\boldsymbol{R}_1}^{K}, \overbrace{\boldsymbol{R}_2}^{2L-1-K}]. \tag{29}$$

2) Construct noise subspace using propagator [21], and the cost function is given by

$$f_R(\gamma, \phi) = \boldsymbol{a}^H(\gamma, \phi)\boldsymbol{\Pi}\boldsymbol{a}(\gamma, \phi), \tag{30}$$

where

$$\boldsymbol{\Pi} = \boldsymbol{Q}_R \left(\boldsymbol{Q}_R^H \boldsymbol{Q}_R\right)^{-1} \boldsymbol{Q}_R^H, \tag{31}$$

$$\boldsymbol{Q}_R = \left[\boldsymbol{P}_R^T, -\boldsymbol{I}_{2L+1-K}\right]^\top, \tag{32}$$

$$\boldsymbol{P}_R = \left(\boldsymbol{R}_1^H \boldsymbol{R}_1\right)^{-1} \boldsymbol{R}_1^H \boldsymbol{R}_2. \tag{33}$$

3) Pairing and estimate γ_k and ϕ_k by solving the following problem,

$$\hat{\gamma}_k, \hat{\phi}_k = \min_{i \in [1,K]} f_R(\bar{\gamma}, \bar{\phi}), \quad k = 1, \ldots, K, \tag{34}$$

where

$$\bar{\gamma} = \frac{1}{2}\left(\alpha_i + \beta_k\right), \tag{35}$$

$$\bar{\phi} = \frac{1}{2}\left(\alpha_i - \beta_k\right), \tag{36}$$

then we can calculate the DOA and range of kth source from (3) and (4),

$$\hat{\theta}_k = \arcsin\left(\frac{-\hat{\gamma}_k \lambda}{2\pi d}\right), \tag{37}$$

$$\hat{r}_k = \frac{\pi d^2 \cos^2\left(\hat{\theta}_k\right)}{\lambda \hat{\phi}_k}. \tag{38}$$

When the range of the kth source does not belong to the Fresnel domain, we discard its range information and judge it as a FFS. In fact, ϕ_k would be close to zero if the kth source is FFS, so we can easily make a distinction between FFSs and NFSs.

D. Summary of the IMOS

After obtaining the array data with a certain number of snapshots, the main stages for the IMOS can be described as follows:

Step 1: Construct $\boldsymbol{C}_1$ and $\boldsymbol{C}_2$, and partition them according to (20).

Step 2: Estimate α_k and β_k from the phase of the K roots of the polynomial $p_\alpha(z_\alpha)$ and $p_\beta(z_\beta)$ respectively nearest to the unit circle in the z-plan in accordance with (26)(27),

$$p_\alpha\left(z_\alpha\right) = z_\alpha^{2(L-1)} g_1^H\left(z_\alpha\right) Q_1 \left(Q_1^H Q_1\right)^{-1} Q_1^H g_1\left(z_\alpha\right), \tag{39}$$

$$p_\beta\left(z_\beta\right) = z_\beta^{2(L-1)} g_2^H\left(z_\beta\right) Q_2 \left(Q_2^H Q_2\right)^{-1} Q_2^H g_2\left(z_\beta\right), \tag{40}$$

where $g_1\left(z_\alpha\right) = \left[z_\alpha^{L-1}, \ldots, 1, \ldots, z_\alpha^{-(L-1)}\right]$, $g_2\left(z_\beta\right) = \left[z_\beta^{L-1}, \ldots, 1, \ldots, z_\beta^{-(L-1)}\right]$, $z_\alpha = e^{-2j\alpha}$, $z_\beta = e^{-2j\beta}$.

Step 3: Construct and partition $\boldsymbol{R}$, use (34) to match α_k and β_k, obtain γ_k and ϕ_k through (35) (36) at the same time.

Step 4: Calculate DOA and range of kth source from (37) (38).

E. Discussion

1) Estimation accuracy: The MOS-based method [20] uses mixed-order statistics as the IMOS. However, the IMOS has no pseudo-orthogonality restriction when estimating NFS parameters, thus it has higher estimation accuracy. For DOAs of FFSs, the error of the IMOS is higher. The TSMUSIC only makes use of eigenvalues and ignores other vectors of the cumulant matrix when estimating the ranges of NFSs. Compared with TSMUSIC, the proposed algorithm has higher accuracy.

2) Computational complexity: Regarding computational complexity, we only consider the major part of the computation that the algorithms consume. According to [11], the TS-MUSIC algorithm needs to construct two large cumulant matrices and decomposes its eigenvalues when estimating the parameters, then perform a one-dimensional spectral search. The computational complexity is $O\{9(2L+1)^2T + 9(4L+1)^2T + (4/3)K(2L+1)^3 + (4/3)K(4L+1)^3 + (180/\Delta\theta)(2L+1)^2\}$. Similarly, the MOS-based method also needs to perform eigenvalue decomposition on a second-order covariance matrix and a constructed fourth-order cumulant matrix. It has a spectral search and a ranges search process, which requires $O\{(2L+1)^2T + 4(2L+1)^3 + (180/\Delta\theta)(2L+1)^2 + 9(2L+1)^2T + 4(2L+1)^3 + (R/\Delta r)(2L+1)^2\}$. The proposed IMOS algorithm also constructs two fourth-order cumulant matrices with smaller dimensions while it introduces the propagator and the rooting method to avoid the eigenvalue decomposition and spectral search with a high computational burden. It requires $O\{18(2L-1)^2T + (2L-1)^3 + (2L-1)^2K + (2L-1)K^2 + (2L+1)^2T + (2L+1)^2K\}$. Obviously, the IMOS has a lower computational cost (see the simulation section for details).

IV. Simulation Results

In this part, we compare the IMOS with TS-MUSIC [11] and MOS-based method [20] and analyze the performance of the novel algorithm. Without loss of general, we assume that the ULA has 13 elements and consider a quarter wavelength inter sensor. The power of all sources to be measured is equal, and the zero mean additive Gaussian white noise is uncorrelated with the sources and array elements. We will use the average root mean square error (RMSE) in 300 independent Monte Carlo simulations to analyze the DOAs and ranges of NFSs and FFSs under different signal-to-noise ratio (SNR) or snapshots number. The SNR of the kth signal is defined as $10\log_{10}(\sigma_k^2/\sigma_n^2)$. The DOA and range are in rad and wavelength respectively.

In the first simulation, we consider one NFS and one FFS located at $(17^\circ, 3\lambda)$ and $(25^\circ, +\infty)$ respectively with equal power. Here, the SNR is varied from 0dB to 30dB and the snapshots number T=200 is an invariant value.

Fig. 2 and Fig. 3 show the RMSEs versus the SNR of estimated DOAs and range individually, including NFS and FFS. Compared with the other methods, the IMOS has better performance in estimating the parameters of NFS. For the FFS, the IMOS is better than TS-MUSIC in DOA estimation, and

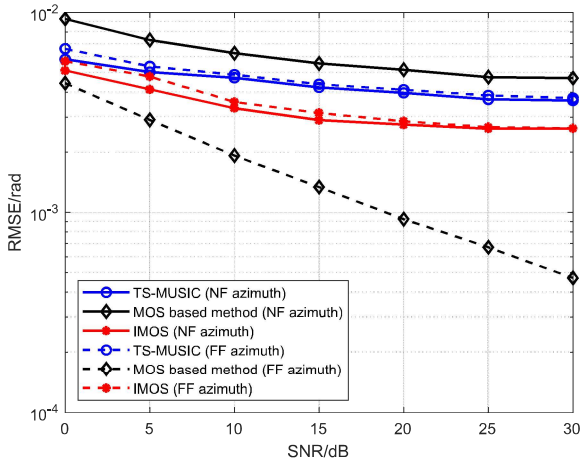

Figure 2. RMSEs of estimated DOAs for NFS and FFS versus SNR (T=200).

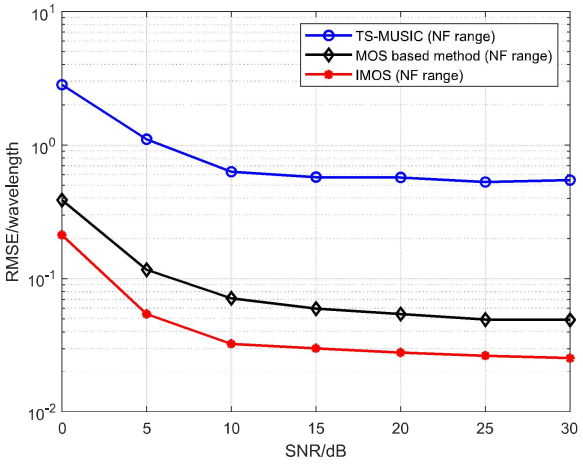

Figure 3. RMSEs of estimated ranges for NFS versus SNR (T=200).

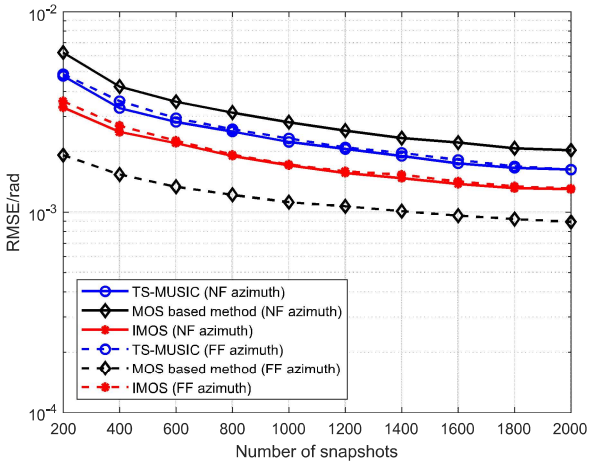

Figure 4. RMSEs of estimated DOAs for NFS and FFS versus snapshots number (SNR=10dB).

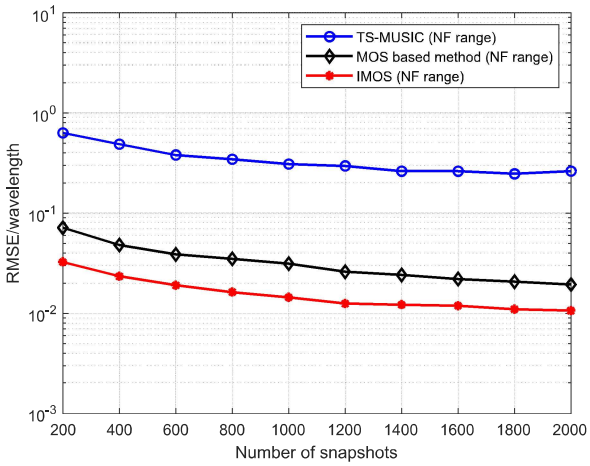

Figure 5. RMSEs of estimated ranges for NFS versus snapshots number (SNR=10dB).

the MOS-based method utilizing second-order statistics has less errors in the ideal case. However, it is noted that the MOS-based method has the worst accuracy of the three algorithms when estimating the DOA of the NF target.

In the second simulation, the performance of the above methods is assessed versus the number of snapshots when we fix SNR=10dB and the number of snapshots is varied from 200 to 2000. The RMSEs of estimated DOAs and range are displayed in Fig. 4 and Fig. 5, respectively. From the figures, we can see that the results are similar to the first simulation. For the NFS, the IMOS has better convergence accuracy regardless of the DOAs or range.

Finally, the third simulation is conducted to compare the computational consumption of the above algorithms. We assume that the number of spectral searchs is 20001 as [11]. The number of targets is set to 2, although its impact on the computational consumption can be almost ignored. Fig. 6 shows the change of computations (flops) with the number of sensors when the number of snapshots is 400, and Fig. 7 shows the change of computations with the number of snapshots when the number of sensors is 15. It can be seen from the figures that the IMOS has the lowest computational consumption among the three, especially when the number of snapshots is small. These results are consistent with the discussion in Section III-E.

V. Conclusion

In this paper, we consider the localization for the mixed sources using the ULA. To combat the issues caused by separating the DOA and range information of the sources or estimating the parameters of FFSs and NFSs separately, an integrated localization method based on mixed-order statistic is proposed. We extract the electrical angles of the constructed cumulant matrices using the propagator and rooting methods, then use the second-order statistics for matching. The novel

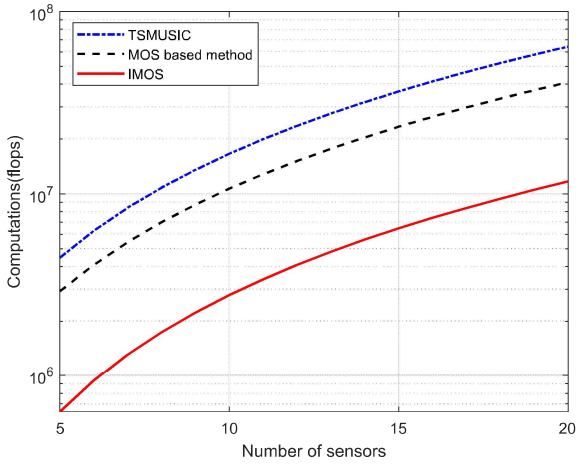

Figure 6. Computational consumption of algorithms versus the number of sensors.

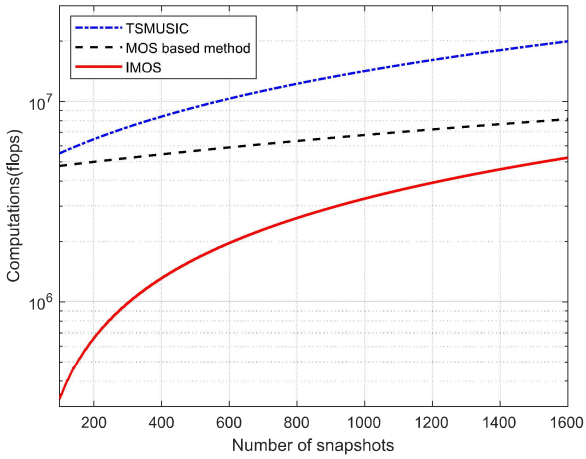

Figure 7. Computational consumption of algorithms versus the number of snapshots.

method has higher computational efficiency while enabling accurate estimation of sources compared to traditional methods, which is demonstrated by several simulation experiments at last.

REFERENCES

[1] H. Krim and M. Viberg, "Two decades of array signal processing research: the parametric approach," *IEEE Signal Processing Magazine*, vol. 13, no. 4, pp. 67–94, 1996.

[2] R. Schmidt, "Multiple emitter location and signal parameter estimation," *IEEE Transactions on Antennas and Propagation*, vol. 34, no. 3, pp. 276–280, 1986.

[3] R. Roy and T. Kailath, "Esprit-estimation of signal parameters via rotational invariance techniques," *IEEE Transactions on Acoustics, Speech, and Signal Processing*, vol. 37, no. 7, pp. 984–995, 1989.

[4] C. M. S. See and A. B. Gershman, "Direction-of-arrival estimation in partly calibrated subarray-based sensor arrays," *IEEE Transactions on Signal Processing*, vol. 52, no. 2, pp. 329–338, 2004.

[5] Q. Shen, W. Liu, W. Cui, S. Wu, and P. Pal, "Simplified and enhanced multiple level nested arrays exploiting high-order difference co-arrays," *IEEE Transactions on Signal Processing*, vol. 67, no. 13, pp. 3502–3515, 2019.

[6] R. N. Challa and S. Shamsunder, "High-order subspace-based algorithms for passive localization of near-field sources," in *Conference Record of the Twenty-Ninth Asilomar Conference on Signals, Systems and Computers*, vol. 2. IEEE, 1995, pp. 777–781.

[7] W. Zhi and M. Y. Chia, "Near-field source localization via symmetric subarrays," in *2007 IEEE International Conference on Acoustics, Speech and Signal Processing-ICASSP'07*, vol. 2. IEEE, 2007, pp. II–1121.

[8] E. Grosicki, K. Abed-Meraim, and Y. Hua, "A weighted linear prediction method for near-field source localization," *IEEE Transactions on Signal Processing*, vol. 53, no. 10, pp. 3651–3660, 2005.

[9] J. Liang and D. Liu, "Passive localization of near-field sources using cumulant," *IEEE Sensors Journal*, vol. 9, no. 8, pp. 953–960, 2009.

[10] C. Guanghui, Z. Xiaoping, J. Shuang, Y. Anning, and L. Qi, "High accuracy near-field localization algorithm at low snr using fourth-order cumulant," *IEEE Communications Letters*, vol. 24, no. 3, pp. 553–557, 2019.

[11] J. Liang and D. Liu, "Passive localization of mixed near-field and far-field sources using two-stage music algorithm," *IEEE Transactions on Signal Processing*, vol. 58, no. 1, pp. 108–120, 2009.

[12] J. He, M. Swamy, and M. O. Ahmad, "Efficient application of music algorithm under the coexistence of far-field and near-field sources," *IEEE Transactions on Signal Processing*, vol. 60, no. 4, pp. 2066–2070, 2011.

[13] J. Jiang, F. Duan, J. Chen, Y. Li, and X. Hua, "Mixed near-field and far-field sources localization using the uniform linear sensor array," *IEEE Sensors Journal*, vol. 13, no. 8, pp. 3136–3143, 2013.

[14] J. Jiang, F. Duan, and X. Wang, "An efficient classification method of mixed sources," *IEEE Sensors Journal*, vol. 16, no. 10, pp. 3731–3734, 2016.

[15] K. Wang, L. Wang, J. Shang, and X. Qu, "Mixed near-field and far-field source localization based on uniform linear array partition," *IEEE Sensors Journal*, vol. 16, no. 22, pp. 8083–8090, 2016.

[16] G. Liu and X. Sun, "Two-stage matrix differencing algorithm for mixed far-field and near-field sources classification and localization," *IEEE Sensors Journal*, vol. 14, no. 6, pp. 1957–1965, 2014.

[17] G. Liu and X. Sun, "Spatial differencing method for mixed far-field and near-field sources localization," *IEEE Signal Processing Letters*, vol. 21, no. 11, pp. 1331–1335, 2014.

[18] A. M. Molaei, B. Zakeri, and S. M. H. Andargoli, "Passive localization and classification of mixed near-field and far-field sources based on high-order differencing algorithm," *Signal Processing*, vol. 157, pp. 119–130, 2019.

[19] A. M. Molaei, B. Zakeri, and S. M. H. Andargoli, "High-performance localization of mixed fourth-order stationary sources based on a spatial/temporal full esprit-like method," *Signal Processing*, vol. 171, p. 107468, 2020.

[20] Z. Zheng, J. Sun, W. Wang, and H. Yang, "Classification and localization of mixed near-field and far-field sources using mixed-order statistics," *Signal Processing*, vol. 143, pp. 134–139, 2018.

[21] W. Zuo, J. Xin, N. Zheng, and A. Sano, "Subspace-based localization of far-field and near-field signals without eigendecomposition," *IEEE Transactions on Signal Processing*, vol. 66, no. 17, pp. 4461–4476, 2018.

[22] Z. Zheng, M. Fu, D. Jiang, W. Wang, and S. Zhang, "Localization of mixed far-field and near-field sources via cumulant matrix reconstruction," *IEEE Sensors Journal*, vol. 18, no. 18, pp. 7671–7680, 2018.

[23] B. Wang, Y. Zhao, and J. Liu, "Mixed-order music algorithm for localization of far-field and near-field sources," *IEEE Signal Processing Letters*, vol. 20, no. 4, pp. 311–314, 2013.

[24] J. S. Aranjo and S. Marcos, "Statistical analysis of the propagator method for doa estimation without eigendecomposition," in *Proceedings of 8th Workshop on Statistical Signal and Array Processing*. IEEE, 1996, pp. 570–573.

[25] S. Marcos, A. Marsal, and M. Benidir, "The propagator method for source bearing estimation," *Signal Processing*, vol. 42, no. 2, pp. 121–138, 1995.